

**On-water surface synthesis of electronically coupled 2D polyimide-MoS<sub>2</sub> van der Waals  
heterostructure**

Anupam Prasoorn<sup>1,2</sup>, Hyejung Yang<sup>1</sup>, Mike Hambsch<sup>3</sup>, Nguyen Ngan Nguyen<sup>1,2</sup>, Sein Chung<sup>4</sup>, Alina Müller<sup>1</sup>, Zhiyong Wang<sup>1,2</sup>, Tianshu Lan<sup>1,2</sup>, Philippe Fontaine<sup>5</sup>, Thomas D. Kühne<sup>6,7</sup>, Kilwon Cho<sup>4</sup>, Ali Shaygan Nia<sup>1</sup>, Stefan C. B. Mannsfeld<sup>3</sup>, Renhao Dong<sup>1,8</sup>, Xinliang Feng<sup>1,2\*</sup>

<sup>1</sup>Center for Advancing Electronics Dresden (cfaed) and Faculty of Chemistry and Food Chemistry, Technische Universität Dresden, 01062 Dresden, Germany

<sup>2</sup>Max Planck Institute for Microstructure Physics, Halle (Saale) D-06120, Germany

<sup>3</sup>Center for Advancing Electronics Dresden (cfaed) and Faculty of Electrical and Computer Engineering, Technische Universität Dresden, 01062 Dresden, Germany

<sup>4</sup>Department of Chemical Engineering, Pohang University of Science and Technology, Pohang, 37673 Republic of Korea

<sup>5</sup>Synchrotron SOLEIL, L'Orme des Merisiers, Départementale 128, 91190, Saint-Aubin, France

<sup>6</sup>Center for Advanced Systems Understanding, Helmholtz-Zentrum Dresden-Rossendorf, 02826 Görlitz, Germany

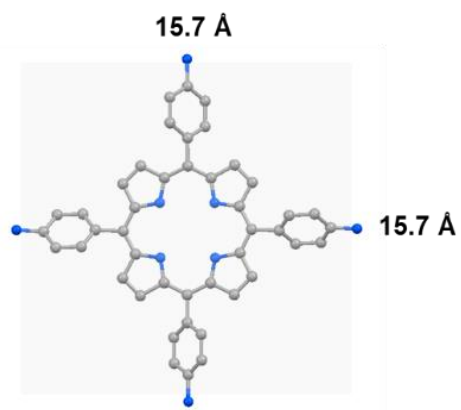
<sup>7</sup>Institute of Artificial Intelligence, Chair of Computational System Sciences, Technische Universität Dresden, 01187 Dresden, Germany

<sup>8</sup>Key Laboratory of Colloid and Interface Chemistry of the Ministry of Education, School of Chemistry and Chemical Engineering, Shandong University, 27 Shandan Road, Jinan 250100, China

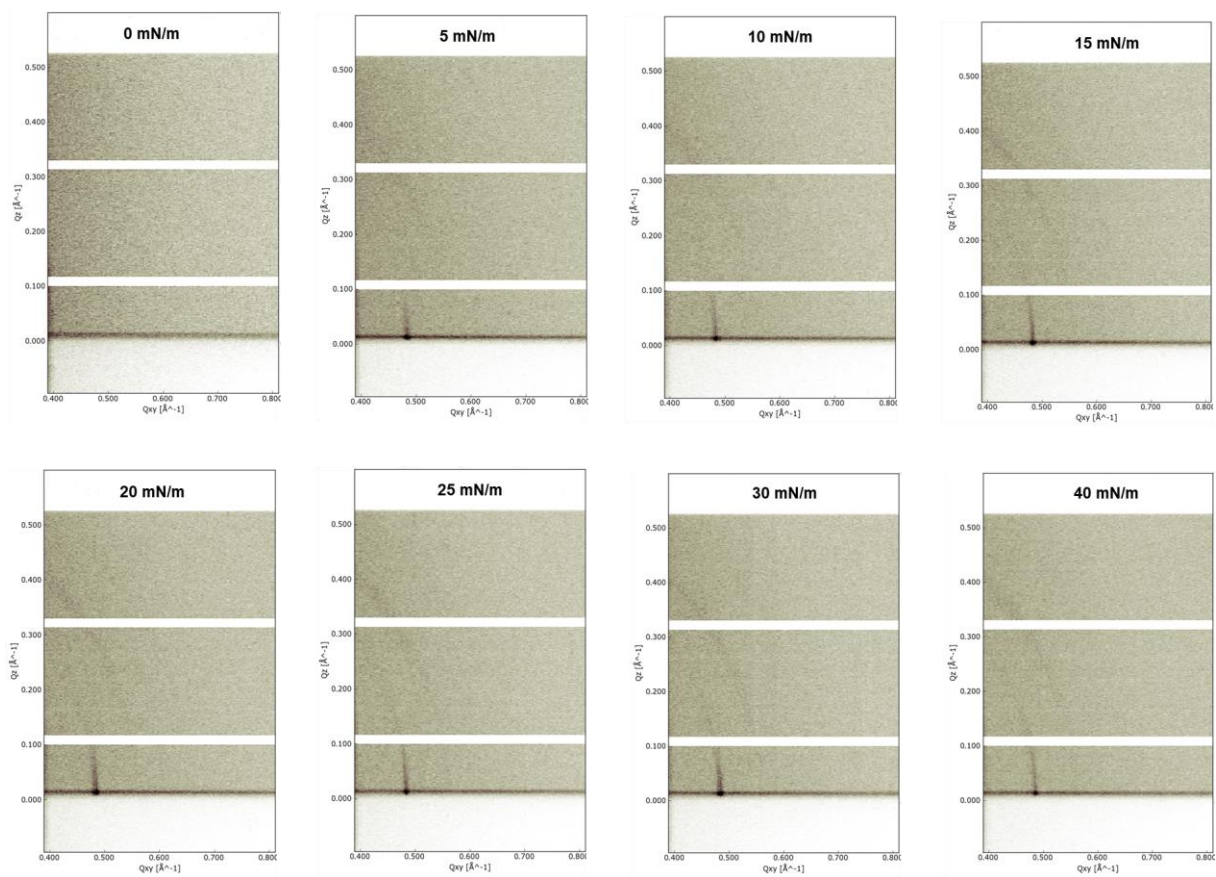
\*E-mail: xinliang.feng@tu-dresden.de

## Table of Contents

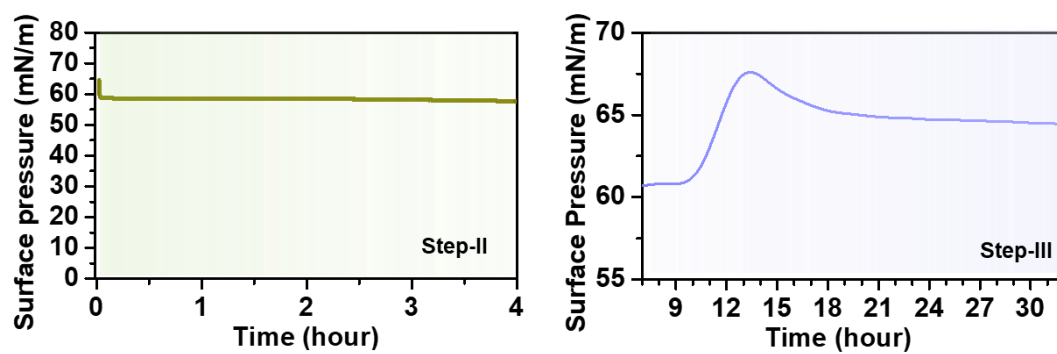
|                              |    |
|------------------------------|----|
| Supplementary Figure 1.....  | 3  |
| Supplementary Figure 2.....  | 4  |
| Supplementary Figure 3.....  | 5  |
| Supplementary Figure 4.....  | 6  |
| Supplementary Figure 5.....  | 7  |
| Supplementary Figure 6.....  | 8  |
| Supplementary Figure 7.....  | 9  |
| Supplementary Figure 8.....  | 10 |
| Supplementary Figure 9.....  | 11 |
| Supplementary Figure 10..... | 12 |
| References.....              | 13 |



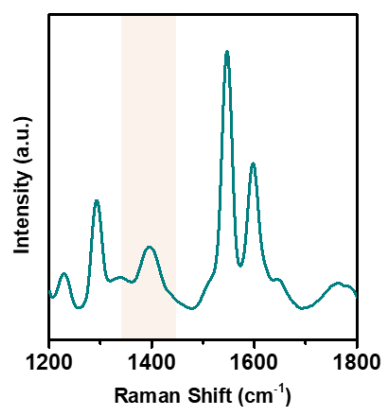
**Supplementary Figure 1.** The pre-organized M1 structure on the water surface exhibits the lattice parameters  $a = b = 13 \text{ \AA}$  and  $\gamma = 90^\circ$ , which are significantly smaller than the size of an individual M1 molecule,  $a = b = 15.7 \text{ \AA}$ .



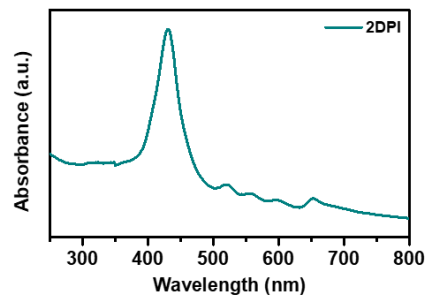
**Supplementary Figure 2.** *In-situ* surface-pressure dependent GIXD measurements of M1 on the water surface.



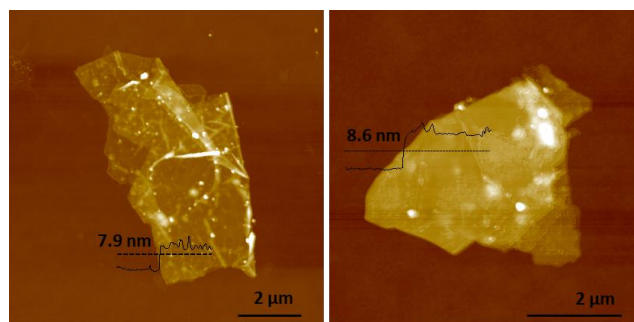
**Supplementary Figure 3.** The evolution of the chemical reaction involving M1 and M2 was monitored using surface pressure measurements versus time over the entire duration of the reaction, i.e., from Step-II to Step-III.



**Supplementary Figure 4.** The Raman spectra of 2DPI show a peak at  $\sim 1403\text{ cm}^{-1}$ , indicating the formation of an imide C-N bond.

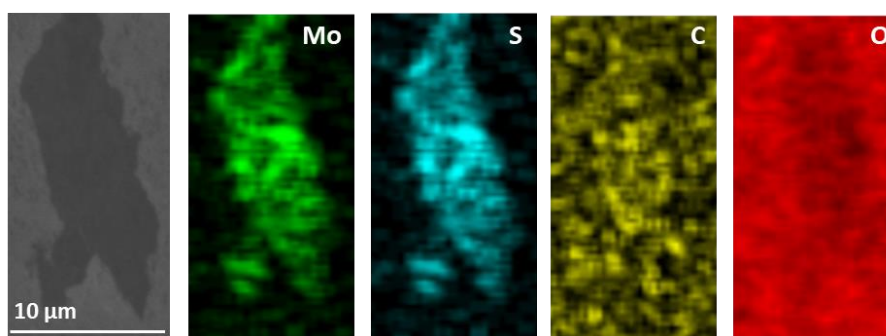


**Supplementary Figure 5.** Solid-state UV-Vis spectra of the as-synthesized 2DPI monolayer.

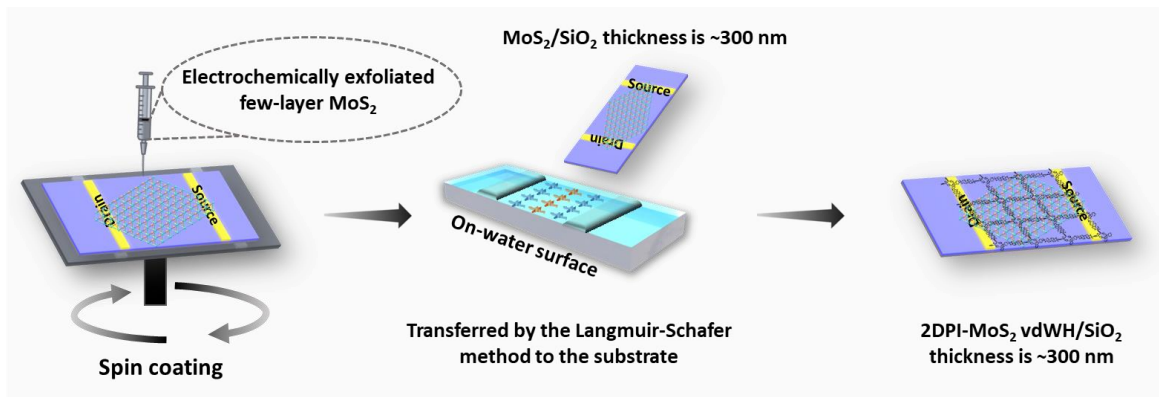


**Supplementary Figure 6.** AFM images of electrochemically exfoliated few-layer MoS<sub>2</sub>.

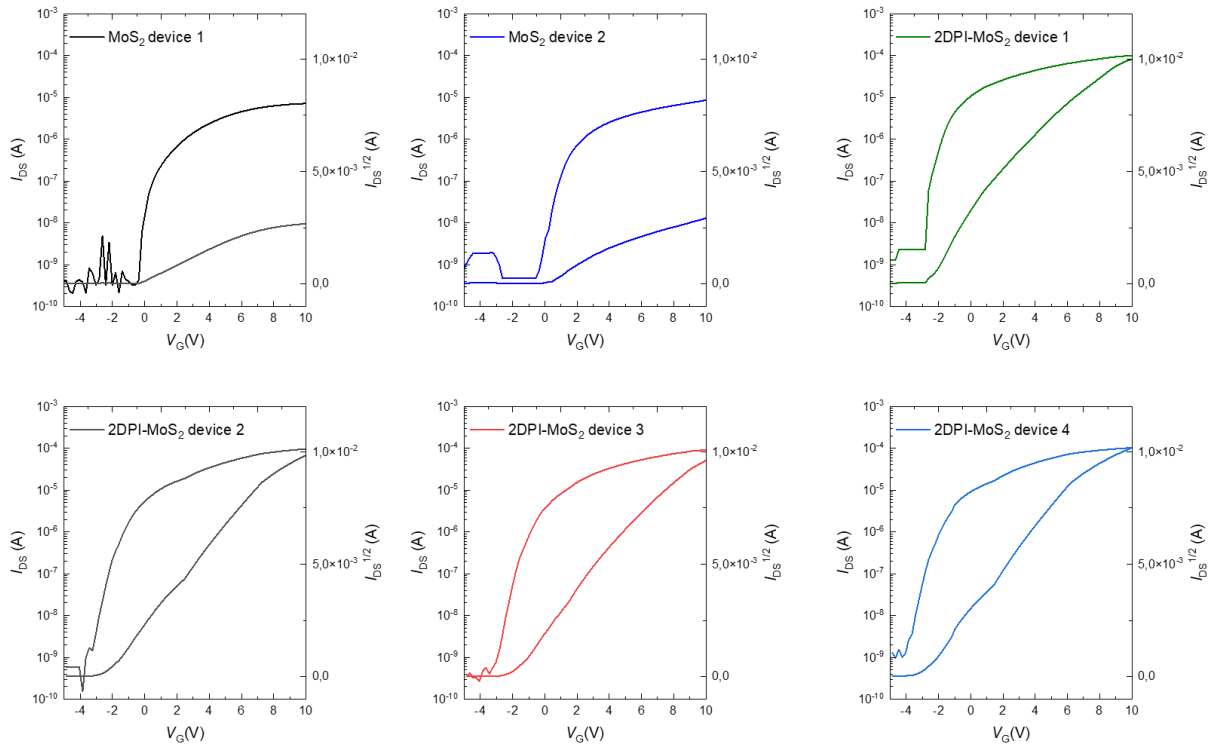




**Supplementary Figure 7.** Elemental mapping of Mo, S, C, and O was performed on the 2DPI-MoS<sub>2</sub> vdWH film.



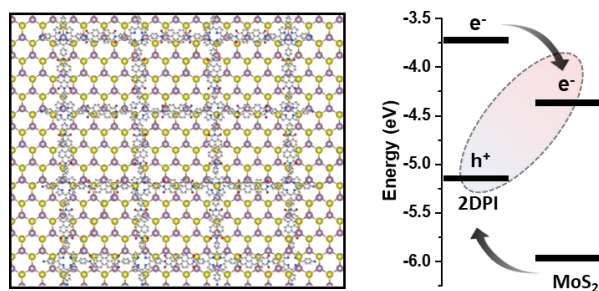
**Supplementary Figure 8.** Schematic of the preparation of 2DPI-MoS<sub>2</sub> vdWH by a wet transfer technique and the device configuration has a  $\frac{1}{4}$  channel length/width ratio, and the SiO<sub>2</sub> thickness is approximately 300 nm.



**Supplementary Figure 9.** FET transfer curve of pristine MoS<sub>2</sub> and 2DPI-MoS<sub>2</sub> vdWH devices.

|                | Mobility         |                       | V <sub>th</sub>  |                       |
|----------------|------------------|-----------------------|------------------|-----------------------|
|                | MoS <sub>2</sub> | 2DPI-MoS <sub>2</sub> | MoS <sub>2</sub> | 2DPI-MoS <sub>2</sub> |
| <b>#1</b>      | 5.4              | 50.0                  | 0.0              | -2.6                  |
| <b>#2</b>      | 8.0              | 34.4                  | 0.5              | -2.5                  |
| <b>#3</b>      |                  | 39.6                  |                  | -1.9                  |
| <b>#4</b>      |                  | 42.3                  |                  | -3.0                  |
| <b>Average</b> | 6.72             | 41.59                 | 0.23             | -2.50                 |

**Supplementary Table T1.** Table of statistical results for FET performance.



**Supplementary Figure 10.** Band alignment of 2DPI-MoS<sub>2</sub> vdWH<sup>1,2</sup>.

### The interactions between 2DPI and MoS<sub>2</sub>

The high crystallinity of the monolayer 2DPI film offers a uniform periodic doping effect on MoS<sub>2</sub> in the 2DPI-MoS<sub>2</sub> vdWH. The Raman spectra of pristine MoS<sub>2</sub> displayed two distinct modes: the E<sub>2g</sub> mode at 385.5 cm<sup>-1</sup>, associated with in-plane vibrations of Mo and S atoms, and the A<sub>1g</sub> mode at 405.07 cm<sup>-1</sup>, related to the out-of-plane vibrations of S atoms. For the 2DPI-MoS<sub>2</sub> vdWH, a red shift of 1.22 cm<sup>-1</sup> was observed in the A<sub>1g</sub> mode of MoS<sub>2</sub>, while the E<sub>2g</sub> mode remained unaltered (Figure 4g). This red shift is attributed to the stronger coupling of the A<sub>1g</sub> mode with electrons in the out-of-plane direction compared to the E<sub>2g</sub> mode. The enhanced FET mobility of the 2DPI-MoS<sub>2</sub> vdWH can be attributed to the synergistic effect of the efficient interfacial electron transfer process and the pronounced suppression of the MoS<sub>2</sub> lattice vibration<sup>3</sup>.

## References

1. Dhakal, K. P. *et al.* Confocal absorption spectral imaging of MoS<sub>2</sub>: optical transitions depending on the atomic thickness of intrinsic and chemically doped MoS<sub>2</sub>. *Nanoscale* **6**, 13028-13035 (2014).
2. Zhang, C. *et al.* Highly fluorescent polyimide covalent organic nanosheets as sensing probes for the detection of 2, 4, 6-trinitrophenol. *ACS Appl. Mater. Interfaces* **9**, 13415-13421 (2017).
3. Wang, C. *et al.* Enhancing the carrier transport in monolayer MoS<sub>2</sub> through interlayer coupling with 2D covalent organic frameworks. *Adv. Mater.*, 2305882 (2023).